Journal of Luminescence 132 (2012) 1819–1823

Contents lists available at SciVerse ScienceDirect

Journal of Luminescence

journal homepage: www.elsevier.com/locate/jlumin

Temperature-dependent photoluminescence of $CuInS_2$ quantum dots

Aimin Shi [a,*], Xiuying Wang [b], Xiangdong Meng [c], Xueyan Liu [b], Haibo Li [c], Jialong Zhao [b,**]

[a] School of Science, Dalian Jiaotong University, Dalian 116028, China
[b] State Key Laboratory of Luminescence and Applications, Changchun Institute of Optics, Fine Mechanics and Physics, Chinese Academy of Sciences, 3888 Dongnanhu Road, Changchun 130033, China
[c] Key Laboratory of Functional Materials Physics and Chemistry of the Ministry of Education, Jilin Normal University, Siping 136000, China

ARTICLE INFO

Article history:
Received 17 November 2011
Received in revised form
4 February 2012
Accepted 14 February 2012
Available online 27 February 2012

Keywords:
$CuInS_2$/ZnS core–shell quantum dots
$CuInS_2$ nanocrystals
Photoluminescence
Temperature-dependent photoluminescence spectroscopy

ABSTRACT

Temperature-dependent photoluminescence (PL) spectroscopy of $CuInS_2$ core and $CuInS_2$/ZnS core–shell quantum dots (QDs) was studied for understanding the influence of a ZnS shell on the PL mechanism. The PL quantum yield and lifetime of $CuInS_2$ core QDs were significantly enhanced after the QD surface was coated with the ZnS shell. The temperature dependences of the PL energy, linewidth, and intensity for the core and core–shell QDs were studied in the temperature range from 92 to 287 K. The temperature-dependent shifts of 98 meV and 35 meV for the PL energies of the QDs were much larger than those of the excitons in their bulk semiconductors. It was surprisingly found that the core and core–shell QDs exhibited a similar temperature dependence of the PL intensity. The PL in the $CuInS_2$/ZnS core–shell QDs was suggested to originate from recombination of many kinds of defect-related emission centers in the interior of the cores.

1. Introduction

Recently copper indium sulfide ($CuInS_2$) colloidal quantum dots (QDs) have been gaining increased interests in optoelectronic applications such as light-emitting diodes (LEDs) and photovoltaic cells because these QDs have lower toxicity than Cd- and Pb-based nanocrystals [1–3]. The $CuInS_2$ QDs have exhibited size-tunable photoluminescence (PL) from the visible to the near-infrared spectral region [4–6]. The PL quantum yield and photostability of the QDs were significantly improved by growing a ZnS shell on the surface of the core [7–15]. Unlike CdSe QDs, a large Stokes shift between the absorption band and PL peak was clearly observed in $CuInS_2$ QDs, suggesting that the broad PL emission was probably related to recombination of donor–acceptor pair (deep defects) [4,6,7]. Recently the PL of $CuInS_2$ core QDs was considered to come from the radiative recombination between an electron in the quantized conduction band state and a hole trapped at either a surface defect or an internal defect. The enhanced PL of $CuInS_2$/ZnS core–shell QDs was explained by an emissive transition involving an extended electron quantized state and a localized hole state because non-radiative surface states were largely passivated by the ZnS shell growth [12,13]. More recently, CuZnInS QDs introducing Zn showed a pronounced tunable PL emission and short PL lifetime [14–16]. However, the PL origin of $CuInS_2$ QDs has not been understood well yet.

The temperature-dependent PL spectroscopy is widely used to study the non-radiative relaxation process and exciton–phonon coupling in colloidal QDs [17–21]. In general, the temperature dependence of the PL emission energy from excitons in QDs should follow that of the band gap in the bulk semiconductors. The variation in the PL intensity as a function of temperature can usually reflect the decrease of the temperature-dependent non-radiative recombination centers or the evolution of the PL mechanism. The variations in the integrated PL intensity for CdSe core and core–shell QDs with increasing temperature are explained by thermal activation of the surface defects/traps and multiple LO phonon-assisted thermal escape of carriers, respectively [21]. The coating of the ZnS shell on CdSe nanocrystals significantly passivated the non-radiative transition centers on the surface of QDs and improved the PL quantum yield. The temperature-dependent optical spectroscopy of $CuInS_2$ crystals has been studied to understand the temperature dependence of the PL bands from excitons and the band gap [22–25]. Therefore, it is necessary to study the effect of the ZnS shell on the optical properties of $CuInS_2$ QDs for understanding the PL origin using temperature-dependent PL spectroscopy.

In this work, we studied the temperature-dependent PL spectra of $CuInS_2$ core and $CuInS_2$/ZnS core–shell QDs. The PL energy, linewidth, and intensity for the QDs as a function of temperature were measured in the temperature range from 92 K to 287 K. The PL origins were discussed.

* Corresponding author. Tel.: +86 411 84106842.
** Corresponding author. Tel.: +86 431 86176029.
E-mail addresses: shiaimin@djtu.edu.cn (A. Shi), zhaojl@ciomp.ac.cn (J. Zhao).

0022-2313/$ - see front matter © 2012 Elsevier B.V. All rights reserved.
doi:10.1016/j.jlumin.2012.02.030

2. Experiment section

2.1. Synthesis of $CuInS_2$ core and $CuInS_2$/ZnS core–shell QDs

$CuInS_2$ core QDs were prepared by thermal decomposition of a mixture of 0.5 mmol (95 mg) of CuI, 0.5 mmol (146 mg) of $In(Ac)_3$ and 5 mL of 1-dodecanethiol (DDT) in a 25 mL three-necked flask. The reaction mixture was degassed under vacuum for 5 min and purged with argon three times. The flask was heated to 120 °C for 10 min until a clear solution was formed. The temperature was then raised to 230 °C. As the temperature increased, the color of the reaction solution progressively changed from colorless to yellow, red, and finally black, indicating nucleation and subsequent growth of $CuInS_2$ QDs. Aliquots were taken at different time intervals to get different size of particles. At the desired size, the reaction was quenched by immersing the flask in a water bath. The collected nanocrystals were purified two times with hexane/acetone co-solvents by centrifugation (6000 rpm, 5 min) and dispersed into hexane for the subsequent measurements.

In the overcoating procedure, 1 mL of the original nanocrystal growth solution was diluted with 4 mL of 1-octadecene (ODE) and then degassed three times. For adgrowth of a ZnS shell, a mixture of 0.3 mmol of zinc stearate, 0.3 mmol of sulfur dissolved in 0.6 mL oleic acid, and 1.5 mL of ODE was added dropwise into the reaction solution at 210 °C for over 20 min. Aliquots were taken at different time intervals to get different sizes of core/shell nanocrystals. The collected nanocrystals were purified two times with hexane/acetone co-solvents by centrifugation (6000 rpm, 5 min) and dispersed into hexane for the subsequent measurements.

2.2. Steady-state fluorescence spectroscopy

The absorption spectra were recorded on a UV-3101PC UV-vis–NIR scanning spectrophotometer (Shimadzu). Steady-state PL spectra were recorded by a Hitachi F-4500 spectrophotometer. The morphology of the nanocrystal samples was characterized by a transmission electron microscope (TEM) (TECNAI G2). The QDs were dispersed in poly-methyl methacrylate (PMMA, molecular weight is 15,000) as a matrix and were then dropped on silicon wafer substrates. The molar ratio of dots/polymer is very small to avoid aggregation of QDs which induced the possibility of Förster resonant energy transfer between differently sized QDs. The temperature-dependent PL was dispersed by a JY-T800 monochromator and detected by a Jobin-Yvon Si-CCD. The QD samples were mounted in a micro-objective cryostat with a controllable temperature range from 92 to 287 K and excited by the 488 nm line of an Ar^+ laser. The laser beam was focused onto the samples by a magnification microscope objective (10×, N.A.=0.25). The laser spot was about 100 μm in diameter.

3. Results and discussion

Fig. 1 shows the absorption and PL spectra of representative $CuInS_2$ core and $CuInS_2$/ZnS core–shell QDs. $CuInS_2$ core QDs with different sizes were prepared by a method that was similar to that in Ref. [12]. The PL peak of $CuInS_2$ core QDs shifted from 680 nm to 760 nm with increasing reaction time up to 30 min, resulting from the quantum size effect. The as-prepared core QDs with a PL wavelength of 680 nm and PL quantum yield of about 5% with the reaction time of 1 min were further used to passivate for improving the PL properties by the growth of the ZnS shell for various durations. The obtained $CuInS_2$/ZnS core–shell QDs exhibited an enhanced PL band with a peak wavelength of 665 nm and a maximum PL quantum yield of 48% after the shell growth for 25 min as seen in Fig. 1. This is similar to the enhancement of as-prepared CdSe/ZnS core–shell QDs [26,27]. During the overgrowth of the ZnS shell, a strong absorption edge around 320 nm and a small PL blue-shift of 15 nm were clearly seen and are shown in Fig. 1, which is related to etching of the core material under shell growth conditions and the associated increase in the degree of spatial confinement [12]. The significant blue-shift was also considered to come from formation of the alloying layer between the $CuInS_2$ core and ZnS shell [10,14–16]. Therefore, the effect of ZnS diffusion on the optical properties of the QDs might be quite small. In addition, the Stokes shifts between the absorption and PL peak were estimated to be 0.52 and 0.48 eV for $CuInS_2$ core and $CuInS_2$/ZnS core–shell QDs, respectively.

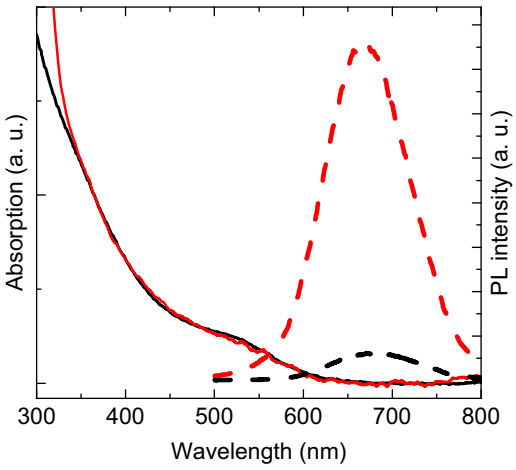

Fig. 1. Absorption (solid lines) and PL (dashed lines) spectra of $CuInS_2$ core (black lines) and $CuInS_2$/ZnS core–shell QDs (red lines). (For interpretation of the references to color in this figure legend, the reader is referred to the web version of this article.)

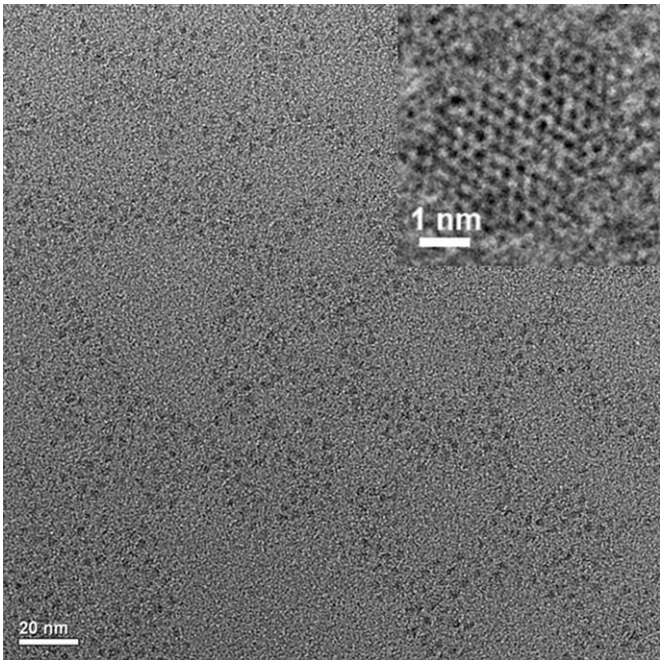

Fig. 2. TEM images of $CuInS_2$/ZnS core–shell QDs. A high resolution TEM image of QDs is shown in the inset of this figure.

The TEM images of $CuInS_2$/ZnS core–shell QDs are shown in Fig. 2. The lattice spacing is clearly seen in the high resolution TEM image, indicating high crystallinity of the QDs. Further the diameters of the core and core–shell QDs were estimated to be

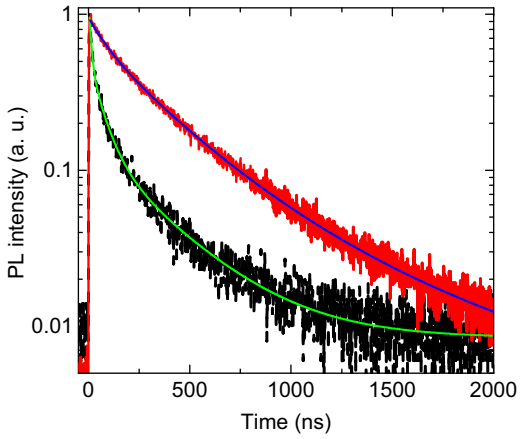

Fig. 3. PL decay curves of $CuInS_2$ core (black dashed line) and $CuInS_2$/ZnS core–shell QDs (red solid line). The solid green and blue lines represent fitting curves. (For interpretation of the references to color in this figure legend, the reader is referred to the web version of this article.)

2.8 and 4.0 nm by TEM images, respectively. This indicated that the $CuInS_2$ cores were coated with about two monolayers of the ZnS shell.

The PL decay curves of $CuInS_2$ core and $CuInS_2$/ZnS core–shell QDs are shown in Fig. 3. The PL decays are not single-exponential, indicating the existence of several emission centers in the QDs. Based on nonlinear least squares, the decay traces of the samples were fitted with a tri-exponential function: $I(t)=A_1\exp(-t/\tau_1)+A_2\exp(-t/\tau_2)+A_3\exp(-t/\tau_3)$, where A_1, A_2, and A_3 are fractional contributions of PL decay lifetimes τ_1, τ_2, and τ_3, respectively. The fitting parameters A_1, A_2, A_3, τ_1, τ_2, and τ_3 were obtained to be 0.81, 0.38, 0.14, 10.3 ns, 64.9 ns, and 321.8 ns for $CuInS_2$ core QDs and 0.25, 0.57, 0.13, 85.5 ns, 303.2 ns, and 723.3 ns for $CuInS_2$/ZnS core–shell QDs, respectively. The average lifetime τ_{ave} was determined by the expression $\tau_{ave}=(A_1\tau_1^2+A_2\tau_2^2+A_3\tau_3^2)/(A_1\tau_1+A_2\tau_2+A_3\tau_3)$. The average times τ_{ave} were obtained to be 205.3 ns for $CuInS_2$ core QDs and 426.1 ns for $CuInS_2$/ZnS core–shell QDs, respectively. The latter one is consistent with the long PL lifetime of 500 ns in Ref. [12]. It is known that there are amounts of defects or traps as non-radiative recombination centers on the surface of QDs. The ZnS shell growth significantly decreases the number of non-radiative traps on the surface of the $CuInS_2$ core QDs, enhancing the PL intensity and lifetime.

Fig. 4(a) and (b) shows the temperature-dependent PL spectra of $CuInS_2$ cores and $CuInS_2$/ZnS core–shell QDs, respectively, recorded in the temperature range from 92 to 287 K. As seen in Fig. 4(a), the PL intensity of the core QDs quickly decreases as the temperature increases. This means that there are amounts of the non-radiative traps on the surface of the core QDs, causing strong thermal quenching. Surprisingly, the PL intensity of $CuInS_2$/ZnS core–shell QDs also rapidly decreases with increasing temperature as seen in Fig. 4(b), which is slightly different from that of the core QDs. The passivation of the ZnS shell greatly enhanced the PL quantum yield and lifetime, reducing non-radiative recombination centers on the surface of the QDs. Therefore, this indicates that the PL mechanism for ZnS shell coated QDs is not changed by the surface modification. In addition, it is noted that the peak energies of PL emissions for the core and core–shell QDs shift to the red with increasing temperature.

The temperature dependences of the emission peak energy and full width at half maximum (FWHM) of the PL band for $CuInS_2$ core and $CuInS_2$/ZnS core–shell QDs are shown in Fig. 5(a) and (b), respectively. As seen in Fig. 5(a), the change in the PL energy for the core and core–shell QDs is 98 and 35 meV, respectively, in the temperature range from 92 K to 287 K. The

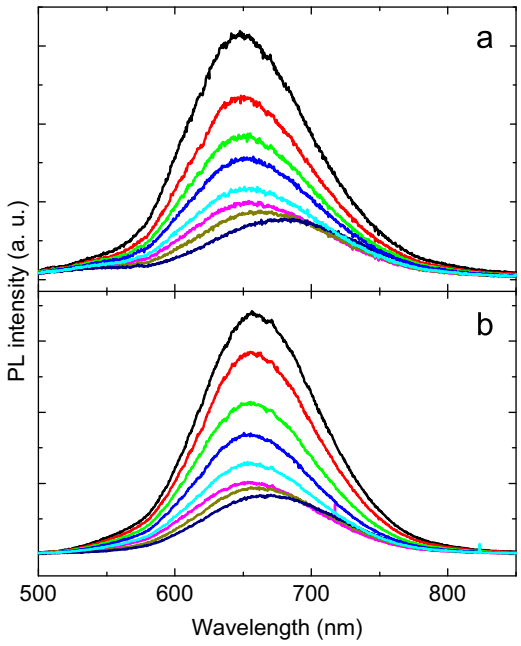

Fig. 4. PL spectra of $CuInS_2$ core (a) and $CuInS_2$/ZnS core–shell QDs (b) at different temperatures 92, 115, 138, 161, 185, 205, 249, and 287 K (from top to bottom) under excitation at 488 nm.

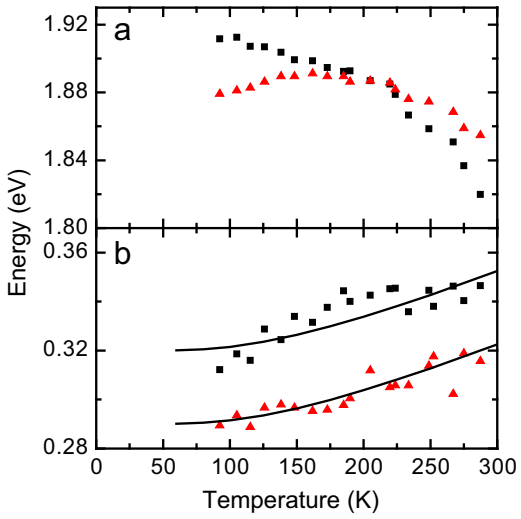

Fig. 5. Temperature dependence of PL emission peak energy (a) and FWHM (b) of $CuInS_2$ core (black solid squares) and $CuInS_2$/ZnS core–shell QDs (red solid triangles). The solid lines in (b) represent theoretical curves with parameters described in the text. (For interpretation of the references to color in this figure legend, the reader is referred to the web version of this article.)

peak energies of PL emissions from excitons in $CuInS_2$ crystals were observed to increase with increasing temperature from 8 to 100 K and decrease with increasing temperature from 100 to 300 K in previous reports [22–24]. Such an increase in band gap of I–III–VI semiconductors with increasing temperature was quite anomalous for II–VI semiconductors that the red-shift of emission peak energy resulted from the lattice deformation potential and exciton–phonon coupling. The variation in the band gap in the temperature range from 8 K to 300 K is about 10–20 meV [22–25]. This indicates that the dominant PL emission of our $CuInS_2$ core QDs or $CuInS_2$/ZnS core–shell QDs with a large temperature-dependent energy shift does not come from the recombination of electrons and holes (excitons) or shallow emission centers near the band edge.

As seen in Fig. 5(b), the FWHMs of the PL in $CuInS_2$ core and $CuInS_2$/ZnS core–shell QDs slightly increase with increasing temperature. In general, the temperature dependence of the FWHM at higher temperature due to exciton scattering with LO phonons can be described by the relation [17–21,25]: $\Gamma(T)=\Gamma_{inh}+\Gamma_{LO}/(\exp(E_{LO}/k_BT)-1)$, here Γ_{inh} is the inhomogeneous linewidth that is temperature independent and results from the fluctuation in size, shape, and composition of QDs, Γ_{LO} represents the exciton–LO-phonon coupling coefficient, and E_{LO} is the LO-phonon energy of about 36 meV obtained from Raman spectra of $CuInS_2$ QDs in the previous reports [28,29]. The temperature dependences of the PL FWHM for $CuInS_2$ core and $CuInS_2$/ZnS core–shell QDs are shown with parameters Γ_{inh} and Γ_{LO} of 320 meV and 0.1 meV for $CuInS_2$ core QDs and 290 meV and 0.1 meV for $CuInS_2$/ZnS core–shell QDs, respectively in Fig. 5(b). The Γ_{LO} in the CdSe QDs was obtained to be 48.7 meV, which is smaller than that of about 100 meV in bulk CdSe material due to the confinement of excitonic polarization in small QDs [21]. The exciton–LO phonon coupling coefficient for a higher transition at 3.409 eV in $CuInS_2$ crystals was determined to be 8.9 meV [25]. However, the coefficient of 0.1 meV obtained in this experiment is really too small to be understood. The PL FWHM of the core and core–shell QDs could not be described simply by the electron–phonon coupling for one kind of emission centers. Therefore, this means that the PL could come from recombination of electrons and holes trapped at many kinds of emission centers, disturbing the accurate estimation of the FWHM in $CuInS_2$ QDs.

In order to understand the shell effect on the non-radiative relaxation processes in QDs, we studied the temperature dependence of the integrated PL intensity. The PL quantum yield and photostability of CdSe core QDs were greatly improved by growing a ZnS or CdS shell with a larger band gap to confine electrons and holes into the core [26,27]. Fig. 6 shows the PL intensities of $CuInS_2$ core and $CuInS_2$/ZnS core–shell QDs as a function of the inverse k_BT. The PL intensities are normalized to the PL at the lowest measurement temperature of 92 K. The temperature dependences of the PL intensities for both the $CuInS_2$ core and core–shell QDs do not show a significant difference. In contrast, CdSe nanocrystals exhibited a clear variation in the temperature dependence of the PL intensity after the shell coating. On the other hand, the PL in CdSe QDs was explained as the recombination of excitons or shallow emission centers near the conduction or valence band in the QDs [17–21]. This means that the surface coating of the $CuInS_2$ core QDs did not effectively change the origin of PL centers despite the enhancement of the PL quantum yield and lifetime in the QDs. Cu–Zn–In–S QDs exhibited tunable PL from the visible to the near-infrared spectral region due to Zn diffusion into $CuInS_2$ cores. The enhancements of the PL intensity and lifetime observed in Cu–Zn–In–S QDs were related to the Cu/Zn ratio [15,16]. However, the enhancement of the PL intensity and lifetime cannot be considered to come from the Zn diffusion in $CuInS_2$/ZnS core–shell QDs. Therefore, this suggests that the ZnS shell growth significantly decreases the number of non-radiative traps on the surface of the $CuInS_2$ core QDs and large amounts of defect-related emission centers are still in the interior of the cores.

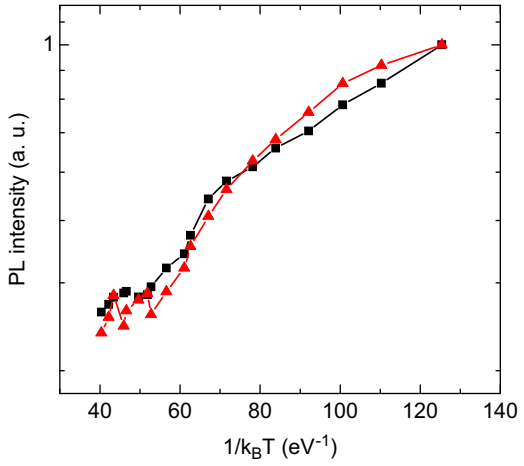

Fig. 6. Integrated PL intensities of $CuInS_2$ core (black solid squares) and $CuInS_2$/ZnS core–shell QDs (red solid triangles) as a function of inverse k_BT. The lines are guides for eyes. (For interpretation of the references to color in this figure legend, the reader is referred to the web version of this article.)

The PL origins in $CuInS_2$, $CuInSe_2$ and $AgInS_2$ QDs have been widely studied [4–6,12,13,30–32]. Most of the PL mechanisms were considered to come from donor–acceptor pairs in these QDs or defect-related emission centers. From the temperature dependence of the PL energy and intensity as seen in Figs. 5(a) and 6, it is impossible for the dominant PL in $CuInS_2$ core and $CuInS_2$/ZnS core–shell QDs to come from the recombination of excitons or the shallow emission centers on the surface of the QDs because the changes in the PL energy for the QDs in the temperature range from 92 K to 287 K are much larger than that of the bulk material. It is known that many defects such as V_{Cu}, V_S, In_{Cu} and so on can be acceptor or donors, resulting in recombination of a donor–acceptor pair or the conduction band–acceptor transition in the luminescence process in $CuInS_2$ QDs. On the basis of the PL FWHM as a function of temperature as seen in Fig. 5(b), the PL in $CuInS_2$ core and $CuInS_2$/ZnS core–shell QDs cannot be considered to come from only one kind of emission centers in the QDs although most of these exterior vacancies or defects were filled and eliminated by coating the ZnS shell. Therefore, the PL in $CuInS_2$/ZnS core–shell QDs probably comes from the recombination of many kinds of emission centers such as vacancies or defects in the interior of the cores, in good agreement with recent results [4–6,12,13].

4. Conclusions

In summary, we have studied the temperature-dependent PL spectra of $CuInS_2$ core and $CuInS_2$/ZnS core–shell QDs. The temperature dependences of PL energy, FWHM and intensity in the QDs were systematically compared with those of the bulk materials or CdSe QDs. The dominant PL in $CuInS_2$/ZnS core–shell QDs could not be considered to come from the recombination of the excitons or shallow emission centers near the conduction or valence band. The experimental results suggested that the PL in the core–shell QDs might originate from the recombination of many kinds of emission centers such as vacancies or defects in the interior of the cores despite the ZnS shell coating. It will be promising to control the crystalline quality of the $CuInS_2$ core QDs and shells to decrease non-radiative recombination processes for improving the performance of $CuInS_2$/ZnS core–shell QDs.

Acknowledgments

This work was supported by the program of CAS Hundred Talents, the National Natural Science Foundation of China (No. 60976049 and No. 51102227). We thank Prof. Renguo Xie for his helpful discussion.

References

[1] S. Coe, W.K. Woo, M. Bawendi, V. Bulovic, Nature 420 (2002) 800.
[2] W.U. Huynh, J.J. Dittmer, A.P. Alivisatos, Science 295 (2002) 2425.
[3] D.V. Talapin, J. Lee, M.V. Kovalenko, E.V. Shevchenko, Chem. Rev. 110 (2010) 389.

[4] S.L. Castro, S.G. Bailey, R.P. Raffaelle, K.K. Banger, A.F. Hepp, J. Phys. Chem. B 108 (2004) 12429.
[5] H. Nakamura, W. Kato, M. Uehara, K. Nose, T. Omata, S. Otsuka-Yao-Matsuo, M. Miyazaki, H. Maeda, Chem. Mater. 18 (2006) 3330.
[6] H.Z. Zhong, Y. Zhou, M.F. Ye, Y.J. He, J.P. Ye, C. He, C.H. Yang, Y.F. Li, Chem. Mater. 20 (2008) 6434.
[7] L. Li, T.J. Daou, I. Texier, T.T.K. Chi, N.Q. Liem, P. Reiss, Chem. Mater. 21 (2009) 2422.
[8] K. Nose, Y. Soma, T. Omata, S. Otsuka-Yao-Matsuo, Chem. Mater. 21 (2009) 2607.
[9] R.G. Xie, M. Rutherford, X.G. Peng, J. Am. Chem. Soc. 131 (2009) 5691.
[10] J. Park, S.W. Kim, J. Mater. Chem. 21 (2011) 3745.
[11] X.S. Tang, W.L. Cheng, E.S.G. Choo, J.M. Xue, Chem. Commun. 47 (2011) 5217.
[12] L. Li, A. Pandey, D.J. Werder, B.P. Khanal, J.M. Pietryga, V.I. Klimov, J. Am. Chem. Soc. 133 (2011) 1176.
[13] D.E. Nam, W.S. Song, H. Yang, J. Colloid Interface Sci. 361 (2011) 491.
[14] Z.A. Tan, Y. Zhang, C. Xie, H.P. Su, J. Liu, C.F. Zhang, N. Dellas, S.E. Mohney, Y.Q. Wang, J.K. Wang, J. Xu, Adv. Mater. 23 (2011) 3553.
[15] W.J. Zhang, X.H. Zhong, Inorg. Chem. 50 (2011) 4065.
[16] J. Zhang, R.G. Xie, W.S. Yang, Chem. Mater. 23 (2011) 3357.
[17] D. Valerini, A. Cretí, M. Lomascolo, L. Manna, R. Cingolani, M. Anni, Phys. Rev. B 71 (2005) 235409.
[18] G. Morello, M. De Giorgi, S. Kudera, L. Manna, R. Cingolani, M. Anni, J. Phys. Chem. C 111 (2007) 5846.
[19] A. Al Salman, A. Tortschanoff, M.B. Mohamed, D. Tonti, F. van Mourik, M. Chergui, Appl. Phys. Lett. 90 (2007) 093104.
[20] S.F. Wuister, A. van Houselt, C. de Mello Doneg, D. Vanmaekelbergh, A. Meijerink, Angew. Chem. Int. Ed. 43 (2004) 3029.
[21] P.T. Jing, J.J. Zheng, M. Ikezawa, X.Y. Liu, S.Z. Lv, X.G. Kong, J.L. Zhao, Y. Masumoto, J. Phys. Chem. C 113 (2009) 13545.
[22] T.M. Hsu, J.H. Lin, Phys. Rev. B 37 (1988) 4106.
[23] K. Yoshino, T. Ikari, S. Shirakata, H. Miyake, K. Hiramatsu, Appl. Phys. Lett. 78 (2001) 742.
[24] M.V. Yakushev, A.V. Mudryi, I.V. Victorov, J. Krustok, E. Mellikov, Appl. Phys. Lett. 88 (2006) 011922.
[25] C.H. Ho, S.F. Lo, P.C. Chi, J. Electrochem. Soc. 157 (2010) H219.
[26] B.O. Dabbousi, J. Rodriguez-Viejo, F.V. Mikulec, J.R. Heine, H. Mattoussi, R. Ober, K.F. Jensen, M.G. Bawendi, J. Phys. Chem. B 101 (1997) 9463.
[27] R. Xie, U. Kolb, J. Li, T. Basche, A. Mews, J. Am. Chem. Soc. 127 (2005) 7480.
[28] M. Uehara, K. Watanabe, Y. Tajiri, H. Nakamura, H. Maeda, J. Chem. Phys. 129 (2008) 134709.
[29] F.M. Courtel, R.W. Paynter, B. Marsan, M. Morin, Chem. Mater. 21 (2009) 3752.
[30] K. Nose, T. Omata, S. Otsuka-Yao-Matsuo, J. Phys. Chem. C 113 (2011) 3455.
[31] T. Ogawa, T. Kuzuya, Y. Hamanaka, K. Sumiyama, J. Mater. Chem. 20 (2010) 2226.
[32] Y. Hamanaka, T. Ogawa, M. Tsuzuki, T. Kuzuya, J. Phys. Chem. C 115 (2011) 1786.